MITSUBISHI ELECTRIC RESEARCH LABORATORIES
http://www.merl.com

Experimental Demonstration of Multi-Pilot Aided Carrier Phase Estimation for DP-64QAM and DP-256QAM

Pajovic, M.; Millar, D.S.; Koike-Akino, T.; Parsons, K.; Savory, S.J.; Maher, R.; Lavery, D.; Bayvel, P.; Paskov, M.; Alvarado, A.; Thomsen, B.C.

TR2015-104 September 2015

Abstract

We present a statistical inference based multi-pilot aided CPE algorithm and analyze its performance via simulations. We experimentally verify LDPC coded back-to-back performance using 10 GBd DP-64QAM and DP-256QAM modulation, with transmitter and receiver linewidths of 100 kHz.

2015 European Conference on Optical Communication (ECOC)

Experimental Demonstration of Multi-Pilot Aided Carrier Phase Estimation for DP-64QAM and DP-256QAM

Milutin Pajovic[1], David S. Millar[1], Toshiaki Koike-Akino[1], Robert Maher[2], Domaniç Lavery[2], Alex Alvarado[2], Milen Paskov[2], Keisuke Kojima[1], Kieran Parsons[1], Benn C. Thomsen[2], Seb J. Savory[2] and Polina Bayvel[2]

(1) Mitsubishi Electric Research Labs., 201 Broadway, Cambridge, MA, 02139, USA, pajovic@merl.com
(2) Optical Networks Group, University College London (UCL), Torrington Place, London, WC1E 7JE, UK

Abstract *We present a statistical inference based multi-pilot aided CPE algorithm and analyze its performance via simulations. We experimentally verify LDPC coded back-to-back performance using 10 GBd DP-64QAM and DP-256QAM modulation, with transmitter and receiver linewidths of 100 kHz.*

Introduction

The need to increase spectral efficiency in coherent optical transmission systems has led to significant interest in high order quadrature amplitude modulation (QAM) formats. One of the difficulties associated with dense modulation formats is their sensitivity to phase noise, and carrier phase estimation (CPE) has become an increasing problem. Blind CPE algorithms, such as the Viterbi and Viterbi algorithm[1], are unsuitable for systems employing dense modulation formats. Consequently, a variety of approaches for CPE have been proposed. The blind phase search (BPS) algorithm[2] provides excellent performance but at very high computational cost. Alternatively, low complexity feedback only decision-directed CPE (DD-CPE)[3] requires sequential processing on a symbol-by-symbol level. A two-stage approach[4] has been studied recently, first coarsely estimating the phase with one algorithm and then after phase unwrapping refining the estimates with a more accurate method. Machine learning methods such as particle filtering[8] for amplitude and phase noise estimation have also been recently explored.

In this paper, we analyze the performance of our recently proposed multi-pilot aided CPE algorithm[6]. This method is based on statistical inference, is of moderate complexity, and is suitable for block-based parallel implementation in hardware. We test this method with DP-64QAM and DP-256QAM via simulations and experiments.

Multi-Pilot CPE Algorithm

We assume all channel impairments except phase noise are compensated and the received signal at discrete time n is given by

$$y_n = x_n e^{j\theta_n} + v_n, \ \ v_n \sim \mathcal{CN}(0, \sigma^2), \qquad (1)$$

where x_n is the transmitted symbol, σ^2 is the variance of the additive Gaussian noise and θ_n is the phase noise modeled as a Wiener process, i.e.,

$$\theta_n - \theta_{n-1} \sim \mathcal{N}(0, \sigma_{\mathrm{p}}^2), \qquad \sigma_{\mathrm{p}}^2 = 2\pi\Delta\nu T_{\mathrm{s}}, \qquad (2)$$

where $\Delta\nu$ is the combined laser linewidths and T_{s} is the symbol duration.

The pilot symbols aiding CPE are uniformly inserted into the data sequence every N information symbols. The multi-pilot CPE algorithm estimates the phase of an information symbol by employing K pilots preceding and K pilots following that symbol. An example for $K = 2$ is shown in Fig. 1, where CPE of information symbols between pilots p_2 and p_3 is performed with the aid of pilots p_1, p_2, p_3 and p_4.

A block diagram of the multi-pilot CPE algorithm is shown in Fig. 2. The algorithm starts with approximating the posterior distribution $p(\theta_{p_k}|x_{p_k}, y_{p_k})$ of the phase of each pilot with Gaussian distribution whose mean μ_{p_k} is the maximum likelihood phase estimate and the variance $\sigma_{p_k}^2$ is approximated as an observed Fisher information[5]. The initial phase estimates are then smoothed by accounting for phase noise statistics (2). This is achieved by processing the posteriors $p(\theta_{p_k}|x_{p_k}, y_{p_k})$, $k = 1, \ldots, 2K$, through a Kalman filter, yielding means and variances of Gaussian posteriors of pilot symbol phases. We note that $2K = 4$ has been used in this paper, minimizing delay and complexity in the Kalman filter.

The phase θ_n of the n-th information symbol in a block is Gaussian distributed, with mean μ_n which is directly evaluated from the Gaussian

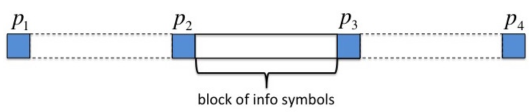

Fig. 1: Multipilot approach for $2K = 4$.

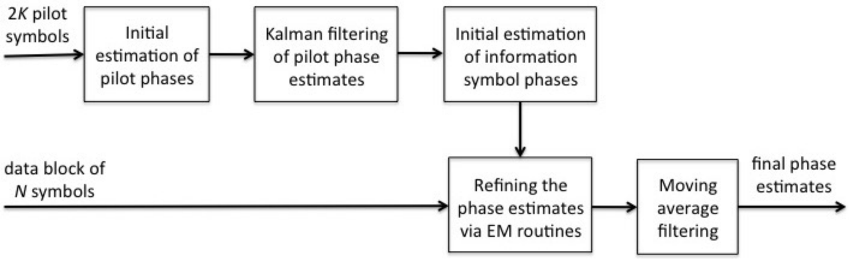

Fig. 2: Block diagram of the CPE of an information block aided with $2K$ pilots.

posteriors corresponding to pilots p_K and p_{K+1}. These means are initial phase estimates and are refined by employing the Expectation Maximization (EM) algortihm on each symbol separately in parallel. The EM routine for the n-th information symbol is initialized with $\hat{\theta}_n^{(0)} = \mu_n$. The k-th iteration evaluates the likelihood $p(x_n|y_n, \hat{\theta}_n^{(k-1)})$ given the phase estimate $\hat{\theta}_n^{(k-1)}$ from the previous iteration. The phase $\hat{\theta}_n^{(k)}$ is then updated from the expected value of the transmitted symbol and the received signal y_n. Two iterations of the EM algorithm were used. Finally, the phase estimates were filtered with a moving average FIR filter.

Simulation

We simulated the variation of required signal-to-noise ratio (RSNR) to achieve a target BER of 10^{-2}. An additive Gaussian white noise (AWGN) channel was used, with purely Lorenzian phase noise. A comparison is made between the algorithm presented in this work, and the decision-directed carrier phase estimation (DD-CPE) algorithm described in[3].

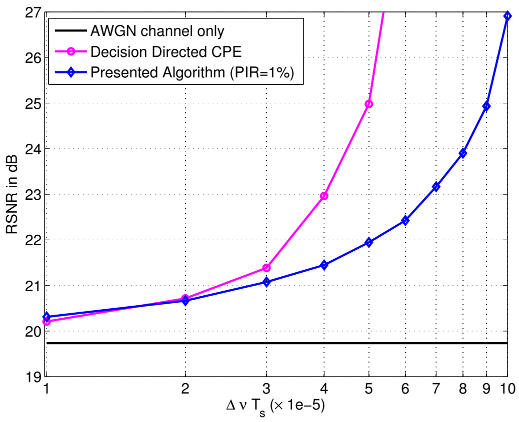

Fig. 3: RSNR to achieve target BER of 10^{-2} for 64QAM.

We note that the DD-CPE operates on a symbol-by-symbol basis, and is unsuitable for hardware implementation due to the requirement of symbol rate feedback. The results of these simulations are shown in Fig. 3 and 4 for, respectively, 64QAM and 256QAM. The RSNR corresponding to the AWGN channel is also indicated in the figures. As can be observed, when 64QAM is used, the proposed method with pilot insertion ratio (PIR) of 1% outperforms the DD-CPE. However, when 256QAM is used, a PIR of 2% is needed to achieve acceptable performance in the considered range of $\Delta\nu T_s$.

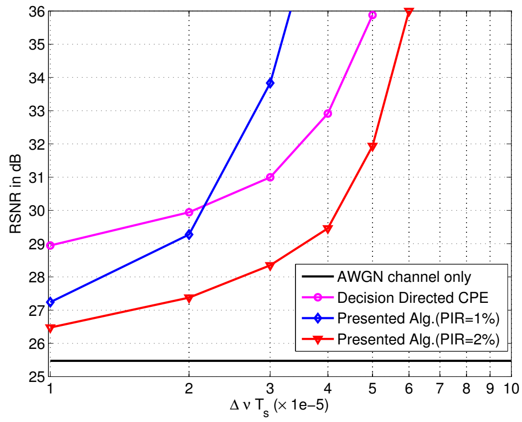

Fig. 4: RSNR to achieve target BER of 10^{-2} for 256QAM.

Experimental Validation

CPE performance was then validated experimentally in a back-to-back configuration for DP-64QAM and DP-256QAM at 10 GBd. The experimental setup used is shown in Fig. 6. A pair of digital-to-analog convertors (DACs) operating at 20 GSa/s were used to generate 64QAM and 256QAM signals at 10 GBd, including 1% pilot symbols. These signals were filtered with a root-raised cosine (RRC) filter with a roll-off factor of 0.1%. After amplification, these signals were applied to an I/Q modulator operating in the linear regime. The optical carrier was generated by an external cavity laser, with a linewidth of 100 kHz. Polarization-multiplexing was emulated passively in the optical domain with a polarization sensitive delay. Noise loading was performed by coupling in a variable power source of amplified spontaneous emission (ASE) noise. A discrete component coherent receiver was used with a bandwidth of 70 GHz, while the local oscillator was an ECL with linewidth of 100 kHz. Quantization was performed using a oscilloscope with 63 GHz bandwidth and 160 GSa/s. Post-processing was then performed offline.

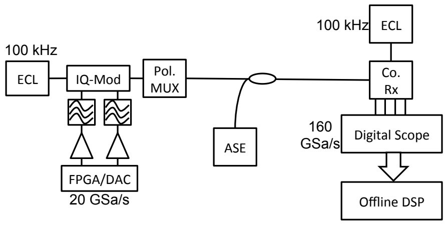

Fig. 5: Setup used for experimental validation.

Our receiver DSP consisted of conventional deskew and normalization blocks, 4th power intradyne frequency estimation, and matched RRC filtering. A 2×2 multiple input multiple output equalizer was used to compensate for polarization rotation, residual intersymbol interference removal and timing phase recovery. The equalizer was initially radially trained for good convergence, before being switched to pilot-aided operation. A constant modulus error term was calculated based on the pilot symbols only, with updating performed using the least mean square algorithm and an error term averaged over 10 pilot symbols. Carrier phase estimation was then performed as previously described. We then calculated bit-wise log-likelihood ratios (LLRs) using a clustering algorithm to account for transmitter distortion. A low-density parity check (LDPC) code with rate 0.78 (28.2% overhead) was then decoded using the sum-product algorithm. We assume the use of an outer hard-decision code with rate 0.93 (7% overhead) and BER threshold of 3×10^{-3}. The systems under consideration therefore have net bit rates of 86.5 Gb/s and 115.5 Gb/s for DP-64QAM and DP-256QAM respectively. This corresponds to intra-channel spectral efficiencies of 8.65 b/s/Hz and 11.55 b/s/Hz respectively, while the total overhead is 38.6%.

The results of our back-to-back characterization are presented in Fig. 6. We note that both formats exhibit a BER floor – around 3×10^{-4} for DP-64QAM and 10^{-2} for DP-256QAM. However, it was noted that we were able to achieve error-free LDPC decoding over 65,536 symbols for both DP-64QAM and DP-256QAM at OSNRs of 17 dB and 23 dB respectively. As we have previously noted[7], performance in the high spectral efficiency asymptote may be limited by electrical impairments rather than optical noise. We therefore note that there are OSNR penalties of 1.9 dB and 2.9 dB at the thresholds of DP-64QAM and DP-256QAM respectively.

Conclusions

We have analyzed the performance of multi-pilot aided carrier phase estimation with DP-64QAM and DP-256QAM. We have noted that this algorithm exhibits good performance with moderate complexity and a fully parallelizable structure. Furthermore, we experimentally demonstrated LDPC coded performance back-to-back using 10 GBd DP-64QAM and DP-256QAM, with transmitter and receiver laser linewidths of 100 kHz, resulting in implementation penalties of 1.9dB and 2.9dB, respectively.

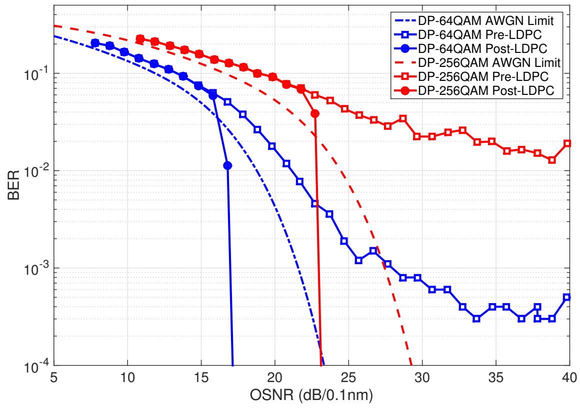

Fig. 6: Experimental results for DP-64QAM and DP-256QAM at 10 GBd, before and after LDPC decoding.

Acknowledgements

This work was in part funded by the UK EPSRC Programme Grant EP/J017582/1, and the Royal Academy of Engineering/ the Leverhulme Trust Senior Research Fellowship held by SJS.

References

[1] A. J. Viterbi et al., "Nonlinear Estimation of PSK-Modulated Carrier Phase with Application to Burst Digital Transmission," IEEE Trans. Inf. Th., Vol. **29**, p. 543 (1983).

[2] I. Fatadin et al., "Blind Equalization and Carrier Phase Recovery in a 16-QAM Optical Coherent System," J. Lightwave Technol., Vol. **27**, p. 3042 (2009).

[3] T. Pfau et al., "Hardware-Efficient Coherent Digital Receiver Concept With Feedforward Carrier Recovery for M-QAM Constellations," J. Lightwave Technol., Vol. **27**, p. 989 (2009).

[4] S. M. Bilal et al., "Dual Stage CPE for 64-QAM Optical Systems Based on a Modified QPSK-Partitioning Algorithm," Photon. Tech. Lett., Vol. **26**, p. 267 (2014).

[5] C. M. Bishop, "Pattern Recognition and Machine Learning (Information Science and Statistics)," Springer-Verlag New York (2006).

[6] M. Pajovic et al., "Multi-Pilot Aided Carrier Phase Estimation for Single Carrier Coherent Systems," Proc. SPPCom 2015.

[7] D. S. Millar et al., "Transceiver-Limited High Spectral Efficiency Nyquist-WDM Systems," Proc. OFC 2015.

[8] D. Zibar et al., "Application of Machine Learning Techniques for Amplitude and Phase Noise Characterization," J. Lightwave Technol., Vol. **33**, p. 1333 (2015).